Department of Pharmacology[1], School of Pharmacy, Fudan University, Shanghai, China; School of Pharmacy[2], Macau University of Science and Technology, Macau

Effects of leonurine on intracerebral haemorrhage by attenuation of peri-hematomal edema and neuroinflammation *via* the JNK pathway

Shizhou Lin[1], Jian Wu[1], Wei Guo[1], Yizhun Zhu[1, 2]

Received May 30, 2016, accepted June 30, 2016

Yizhun Zhu, MD, PhD, School of Pharmacy, Macau University of Science and Technology, Macau
yzzhu@must.edu.mo

Pharmazie 71: 644–650 (2016) *doi: 10.1691/ph.2016.6692*

Perihematomal edema plays a critical role in secondary brain injury in intracerebral hemorrhage (ICH), which is associated with inflammation, hematoma toxicity and oxidative stress. In this work, we investigated the protective effects of leonurine, an alkaloid of *Herbal Leonuri,* and possible mechanisms to provide a basis for a new therapeutic approach for ICH treatment. In *in vivo* studies, we demonstrated for the first time that leonurine treatment substantially decreased perihematomal edema, ameliorated neurobehavioral function deficits, reduced apoptosis and protected injured cerebral tissue after ICH. These benefits appear to be ascribed to leonurine effectively attenuating blood-brain barrier (BBB) breakdown *in vivo*, by inhibiting degradation of hemoglobin and alleviating inflammatory mediator release. In this study, BV-2 cells were exposed *in vitro* to oxyhemoglobin (OxyHb) at a concentration of 10 μM to mimic neuroinflammation after ICH. Consistent with the results of the *in vivo* study, leonurine significantly inhibited OxyHb-induced inflammatory proteins expression in BV-2 cells, mainly through inhibiting the c-Jun N-terminal kinase (JNK) signaling pathway. This is the first time that leonurine is proved to be capable to protect the injured cerebral tissue after ICH, based on alleviating neuroinflammation and attenuating BBB breakdown to ameliorate perihematomal edema.

1. Introduction

Intracerebral haemorrhage (ICH) is a fatal subtype of stroke with high risk of mortality and morbidity (Sacco et al. 2009). Currently, there is no effective strategy that can definitely improve survival rate and life quality for patients suffering from ICH (Adeoye and Broderick 2010). Many studies indicate that secondary brain injury initiated by primary injury (e.g. mass effect and physical disruption) is the key factor of rapid deterioration in ICH(Keep et al. 2012). Secondary brain injury occurs *via* many pathological pathways, including: blood cytotoxicity (Xi et al. 2006); excitotoxicity (Qureshi et al. 2003); oxidative stress and inflammation (Aronowski and Zhao 2011), etc. This pathogenesis ultimately leads to blood-brain barrier disruption and contributes to brain edema formation.

Recent studies suggest that Traditional Chinese Medicine with the function of promoting circulation and removing stasis could serve as an effective treatment for ICH. *Herba Leonuri* can both improve blood circulation and be helpful to *post partum* recovery. The effective ingredient of *Herba Leonuri* is leonurine (SCM-198), whose molecular structure is $C_{14}H_{21}N_3O_5$ and molecular weight is 347.79. According to our previous investigations, leonurine possesses lots of pharmacological functions such as antioxidation, antiapoptosis and cardioprotection (Liu et al. 2009, 2010). It can also suppress the inflammatory effect in HUVEC through inhibiting the NF-kB pathway and regulating mitochondrial function *via* an antiapoptotic mechanism (Liu et al. 2012). However, it remains unclear whether leonurine has a therapeutic effect on ICH and how leonurine functions in ICH-induced injury. Therefore, this paper aimed to investigate the therapeutic effect and mechanisms of leonurine for ICH.

2. Investigations and results

2.1. Leonurine effectively improves the pathological state of ICH in rats

In order to investigate the protective effect of leonurine, we first established a rat model of ICH using the double-injection method. As is shown in Fig. 1A, the ellipse-shaped hematoma was found in the caudatum. As the experiment progressed, leonurine treatment substantially decreased the brain water content (Fig. 1B) and improved neurobehavioral function under the double-blinded condition (Fig. 1C). Using H&E staining, we observed that the ICH-induced rarefaction of cerebral tissue and inflammatory injury was attenuated in leonurine-treated group (Fig. 1D). In addition, obvious apoptotic response was observed in the model group, and leonurine treatment reduced ICH-induced apoptosis significantly (Fig. 1E).

2.2. Attenuation of BBB permeability induced by leonurine

The apparent morphological change of the right brain induced by brain edema (Fig. 1A) prompted us to examine the permeability of BBB via Evans Blue (EB) Analysis. EB content of the treatment group was lower than that of the model group (Table). These data demonstrate the important role of leonurine in supporting BBB maintenance and reducing ICH-induced brain edema.

2.3. Leonurine indirectly protected BBB via altering MMPs expression

We next explored the further mechanism of leonurine-induced regulation of BBB permeability and attenuation of brain edema in ICH. Matrix metalloproteinases (MMPs), in particular MMP-9 and MMP-2, are strongly correlated with leaky BBB and ICH severity in patients (Gu et al. 2012). Thus, we examined MMP-9 and MMP-2 expression induced by ICH and found that MMP-9 and MMP-2 expression was inhibited significantly after leonurine treatment (Fig. 2 A and C).

2.4. Leonurine decreased the degradation of hemoglobin and alleviated inflammatory proteins expression in vivo

In ICH pathogenesis, the expressions of COX-2 and HO-1 increased, which were associated with BBB breakdown. Seventy-two hours

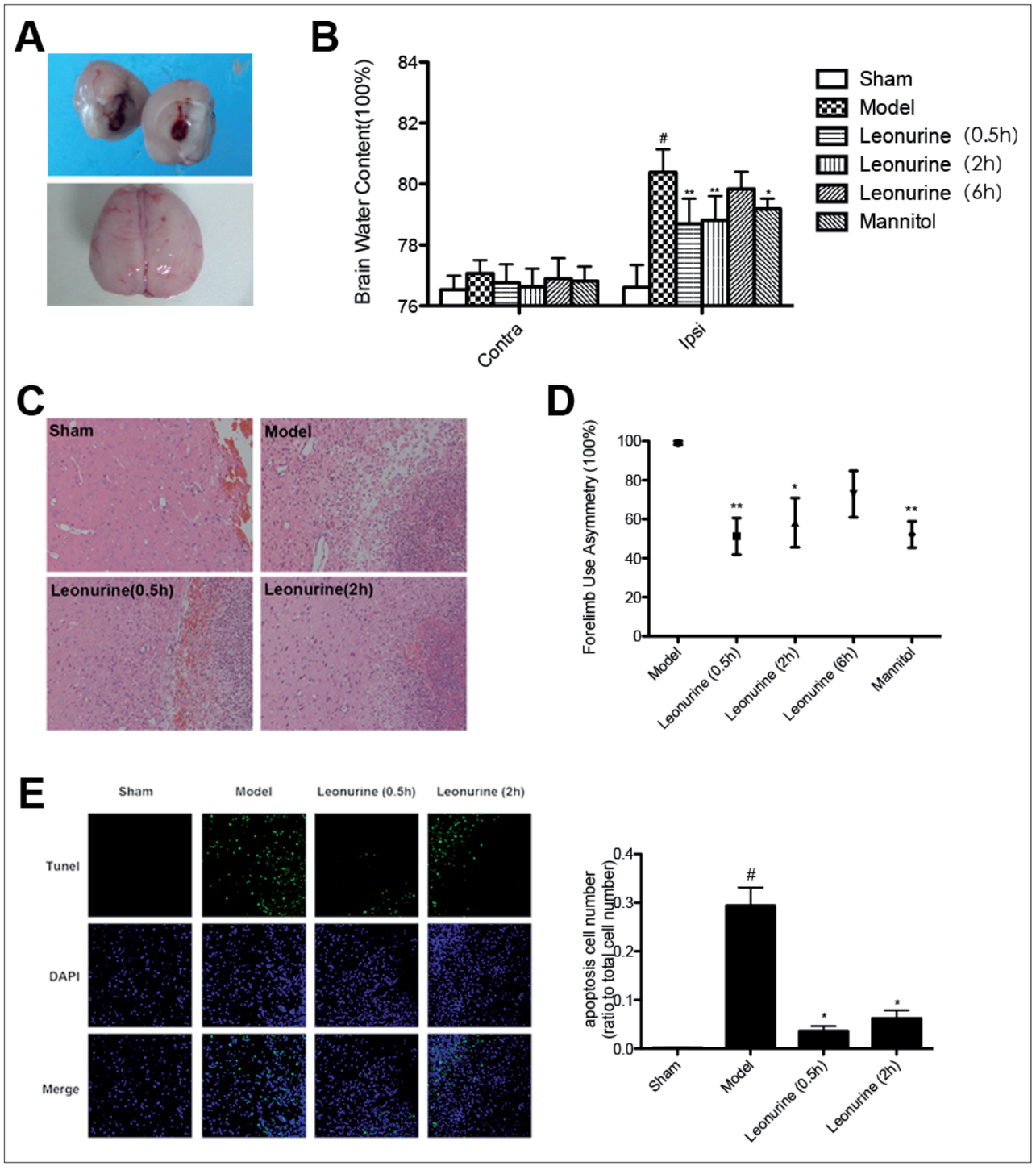

Fig. 1: Leonurine alleviated ICH-induced brain edema, improved neurobehavioral function of SD rats, and suppressed inflammatory infiltration and apoptosis in the perihematoma. (A) The ellipse-shaped hematoma and apparent morphological change of the right brain induced by ICH. (B) Brain water content of contralateral and ipsilateral hemispheres at 3 days after ICH; (C) Forelimb use asymmetry at 3 days after ICH (an infusion of 50 μL autologous whole blood). Data represent mean±SEM of eight to ten rats per group. (D) H&E staining of the brain sections in the perihematoma was performed to observe the morphological change. (E) TUNEL staining for evaluation of cell apoptosis in the perihematoma. The apoptotic cells is represented as the TUNEL-positive cells in each field (n=3 rats/group). Data represent mean±SEM. *P<0.05, **P<0.01 vs. model group. # P<0.05, Tukey's test versus sham group.

after ICH, the expressions of COX-2 and HO-1 were detected by Western Blot assay. As is shown in Fig. 2B, both COX-2 and HO-1 expressions were repressed by leonurine in the treatment group.

The paraffin sections of brain samples were stained by TLR4 antibody and visualized in the perihematoma by a Zeiss digital camera. In the sham group TLR4 expression was not detected and normal cell morphological structure was seen. Three days after ICH, in the model group TLR4 over-expression was observed in the perihematoma. In the leonurine-treated group, TLR4 expression was significantly decreased, and the gap between damaged brain tissues was alleviated (Fig. 2F). Western Blot analysis of TLR4 and MyD88 also demonstrated that elevated levels of these proteins in the model group could be repressed by leonurine treatment, which was consistent with the IHC result (Fig. 2G).

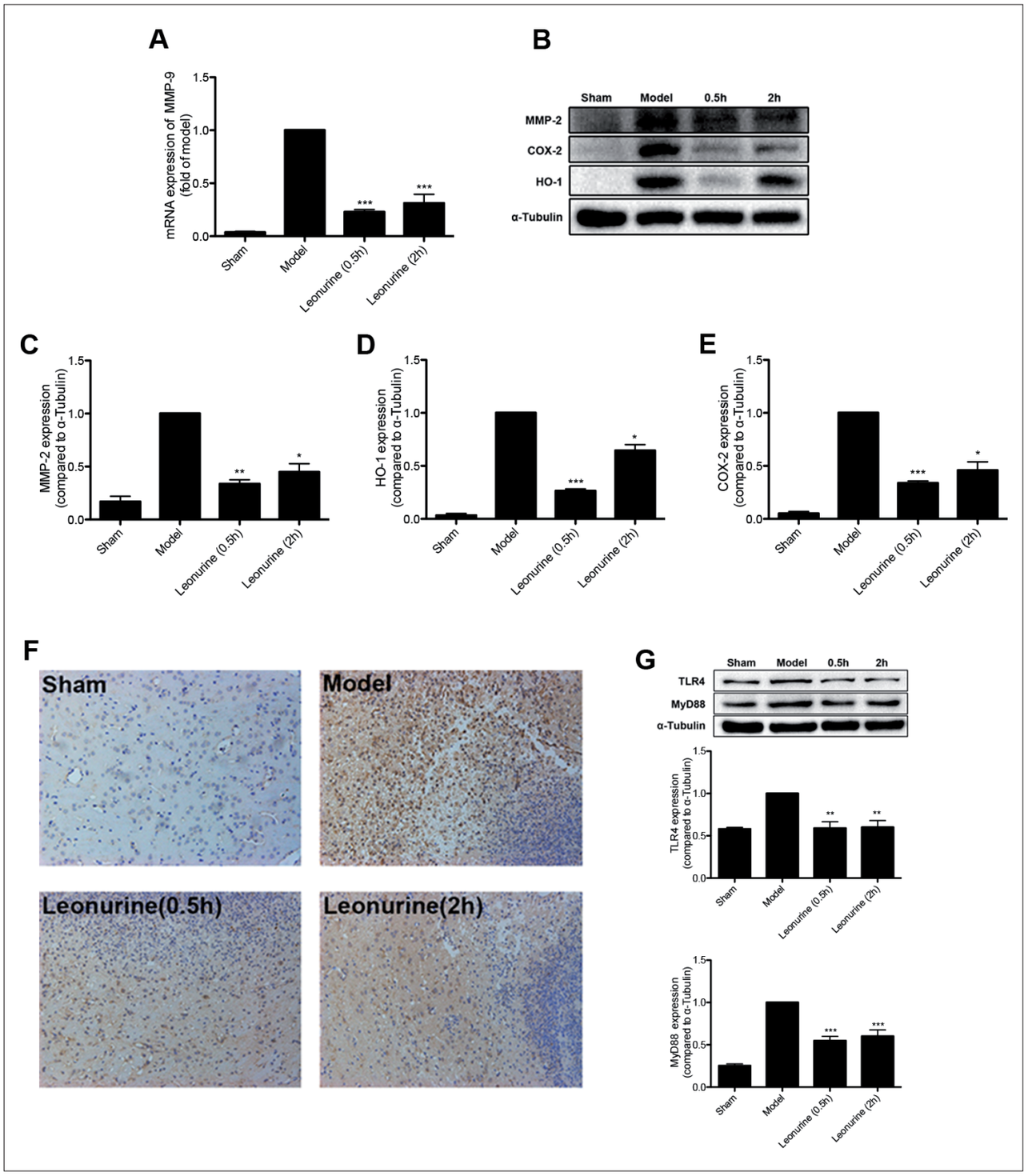

Fig. 2: Leonurine could support BBB maintenance via decreasing MMPs expression and reducing inflammatory injury *in vivo*. (A) RT-PCR for MMP-9 and quantification after normalizing by GADPH (n=6 rats/group). The expressions of MMP-2 (B, C), COX-2 (B, D), HO-1 (B, E), TLR4 and MyD88 (G) were measured by Western blot (n=6 rats/group). (F) Immunohistochemistry. Brain sections were stained with TLR4 antibody to observe TLR4 expression in the perihematoma. Data represent mean±SEM. **P*<0.05, ***P*<0.01, ****P*<0.001 vs. Model group.

2.5. Treatment with leonurine and OxyHb revealed no cytotoxic effect on BV-2 cells

To identify the cytotoxic effect of leonurine and OxyHb on BV-2 cells, we used a CCK-8 assay to measure the viability of BV-2 cells. As shown in Fig. 3, we observed no obvious cytotoxic effect for different concentrations of OxyHb or leonurine on BV-2 cells (Fig. 3A).

2.6. Leonurine inhibited OxyHb-induced proinflammatory mediator release in BV-2 cells

Based on the outstanding protective effects of leonurine *in vivo*, we continued to investigate possible anti-neuroinflammatory mechanism *in vitro*. We first examined inhibitory effects of leonurine on proinflammatory proteins and cytokine release induced by OxyHb in BV-2 cells. Twenty-four hours treatment of BV-2

Table: Leonurine could effectively attenuate BBB disruption at 3 days after ICH *in vivo*

Groups	Sham	Model	Leonurine	
			0.5h	2h
n	6	6	6	6
Dose (mg/Kg)	-	-	15	15
EB content (μ g/g)	1.87±0.15	9.60±0.27#	5.62±0.55**	5.37±0.46**

ICH-induced blood-brain barrier (BBB) permeability was determined by Evans blue leakage method. Data represent mean±SEM of six rats per group. **P<0.01 vs. Model group. # P<0.05,Tukey's test versus Sham group.

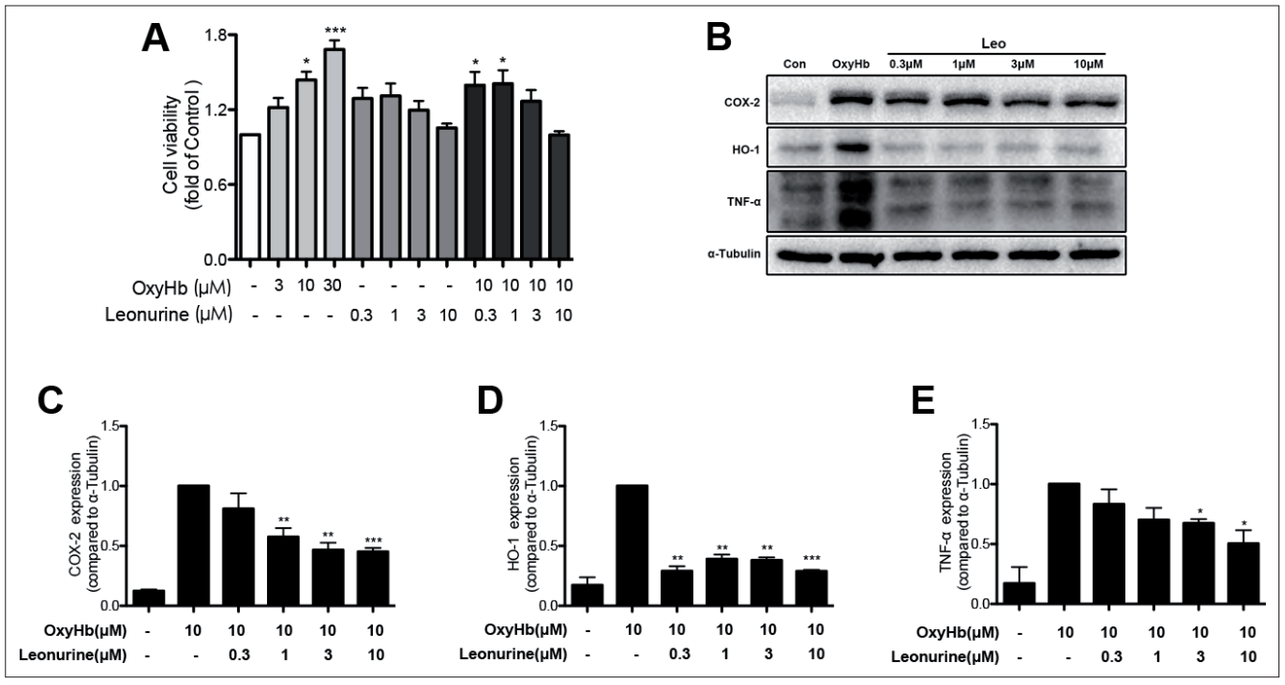

Fig. 3: Lonurine inhibited the degradation of oxyhemoglobin and OxyHb-induced proinflammatory proteins release. (A) Leonurine and oxyhemoglobin (OxyHb) revealed no cytotoxic effect on BV-2 cells. BV-2 cells were treated with different concentrations of leonurine or oxyhemoglobin (OxyHb) for 24 h and then analyzed by CCK-8 assay. Leonurine suppressed protein expression of Cox-2 (B, C), HO-1 (B, D) and TNF-α (B, E) after BV-2 cells were treated with 10 μM OxyHb and different concentrations of leonurine for 24 h. The quantitation represents the average relative ratio of Cox-2, HO-1 and TNF-α to α-tubulin. Data represent mean±SD of three independent experiments. *P<0.05, **P<0.01, ***P<0.001 vs. control group.

cells with leonurine could effectively inhibit OxyHb-induced upregulation of Cox-2 and HO-1 expressions. Exposed to 10 μM OxyHb for 24 h, the production of TNF-α was also suppressed under treatment with 3 μM to 10 μM leonurine in BV-2 cells (Fig. 3B-E).

2.7. Leonurine inhibited activation of JNK pathway induced by OxyHb in BV-2 cells

To determine the optimal time for OxyHb stimulation, we chose 10 μM OxyHb to stimulate BV-2 cells for 5 min to 2 h and used Western Blot Assay to detect the phosphorylation of NF-κB and MAPKs. As shown in Fig. 4B, 10 μM OxyHb could induce NF-κB and MAPKs phosphorylation in a time-dependent manner, and we chose 15 min as the optimal time for OxyHb stimulation (Fig. 4A).

The inhibitory effect of leonurine on NF-κB phosphorylation was not significantly lower than in the OxyHb group, and only 10 μM leonurine could effectively suppress phosphorylation of ERK in BV-2 cells. However, 15 min treatment with 0.3 μM to 10 μM leonurine could significantly inhibit JNK phosphorylation, indicating that leonurine alleviated neuroinflammation and exerted protective effects *via* the c-Jun N-terminal kinase (JNK) signaling pathway, and suppressed NF-κB and ERK pathways indirectly (Fig. 4B-E).

3. Discussion

As a double autologous blood injection is the best choice to mimic ICH, our research used this model to investigate protective effects and mechanisms of leonurine on ICH. The autologous blood was injected in the caudate putamen (0.7 mm anterior to bregma, 3 mm lateral to midline and 5.8 mm deep). The injected volume of blood was 50 μL, which corresponds to the hematoma of volume about 40 mL in human body (Nath et al. 1986). Therefore, it is the moderate size for us to mimic ICH in a rat model.

Perihematomal edema induced by ICH is one of the main reasons to determine secondary brain injury and lead to poor outcome. Hence, the level of brain edema is a criterion to evaluate protective effects after treatments. Extensive researches have documented mannitol, one of the most commonly used osmotic dehydrants in clinic, can reduce the raised intracranial pressure through improving osmotic pressure of plasma (James 2006) and suppress oxygen free radical reaction to protect injured cerebral tissue (Suzuki et al. 1985). Thus, mannitol was chosen as the positive control for study *in vivo*. Our data demonstrated that leonurine treatment substantially decreased perihematomal edema, ameliorated neurobehavioral function deficits and protected injured cerebral tissue after ICH (Fig. 1B and 1C). However, six hours after operation, the leonurine treatment is not effective any longer *in vivo*, indicating that the time window for leonurine treatment should be less than 6 h after

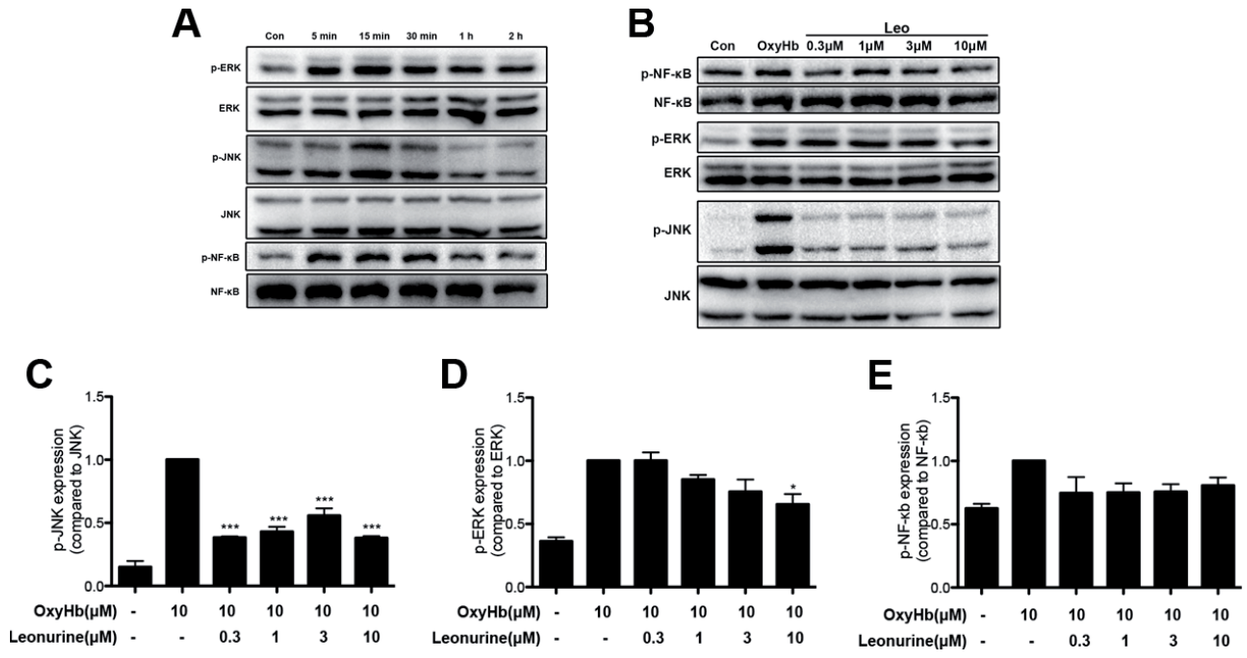

Fig. 4: Leonurine inhibited oxyhemoglobin (OxyHb)-induced c-Jun N-terminal kinase (JNK) phosphorylation in BV-2 cells. (A) Exposure of BV-2 cells to 10μM OxyHb led to a time-dependent phosphorylation of NF-κB, ERK and JNK. (B-E) BV-2 cells were treated with 0.3 to 10 μM leonurine and stimulated by 10 μM OxyHb for 15 min. Leonurine inhibited phosphorylation of ERK (p-ERK), JNK (p- JNK) and NF-κB (p-NF-κB). Data represent mean±SD of three independent experiments. *P<0.05, **P<0.01, ***P<0.001 vs. model group.

ICH. Evans Blue analysis showed that leonurine could effectively attenuate BBB breakdown. Figures 2A and 2C show that leonurine could significantly decrease MMP-9 and MMP-2 expression after ICH. It has been reported that MMPs, in particular MMP-9 and MMP-2, can disrupt continuous tight junctions and degrade extracellular matrix, resulting in increasing permeability of blood-brain barrier and exacerbating brain edema (Yi et al. 2007; Lischper et al. 2010; Yang and Rosenberg 2011; Gu et al. 2012; Jie et al. 2012). Therefore, one possible underlying mechanism is based on supporting BBB maintenance, which leads to alleviation of perihematomal edema after ICH.

Inflammation plays a crucial role in impairing BBB function after ICH. During the pathological progress, the degradation of oxyhemoglobin (OxyHb) from lysed erythrocytes in hematoma causes a series of cytotoxic effects and participates in the formulation of perihematomal edema (Xi et al. 2001). BBB impairment is associated with high levels of TNF-α (Ubenauf 2007). Besides cytokine overexpression, COX-2, induced in response to TNF-α during neourinflammation, is also related with the decrease of tight junctions, which causes BBB disruption (Strazza 2011). These inflammatory mediators are all produced in the downstream signaling transduction pathways of TLR4 (Waleed et al. 2014). *In vivo* experiments proved that the expression of TLR4 and inflammatory mediators were all significantly repressed by leonurine (Fig. 2). This means leonurine exerts protective effects, at least partially, via inhibiting inflammation induced by the degradation of hemoglobin.

Moreover, the underlying mechanisms need further investigation *in vitro*. The degradation of hemoglobin after erythrocyte lysis within the hematoma aggravates ICH-induced inflammatory injury and contributes to BBB disruption. Meanwhile, many studies have stated microglia perform an essential role in immune response and are involved in brain endothelial cells (EC) damage and BBB disruption in stroke (Da 2014). We herein used oxyhemoglobin (OxyHb) as the inflammation inducer to stimulate microglial cells. *In vitro*, BV-2 cells were exposed to OxyHb at a concentration of 10 μM for 24 h to mimic neuroinflammation after ICH. In most cases, 10 μM leonurine exerted best inhibitory effects for the expression of HO-1, COX-2 and TNF-α in BV-2 cells. Besides, 10 μM OxyHb indeed induced phosphorylation of NF-κB and MAPKs, and the level of this progress reaches its maximum after 15 min. We found that 0.3 μM to 10 μM leonurine could significantly inhibit JNK phosphorylation, but partly for NF-κB and ERK. Moreover, recent studies found that neuroinflammatory state activated JNK pathway in microglia, resulting in microglial activation directly and microglial-induced BBB disruption, further leading to cytokine release and amplification of neuroinflammatory response. Taken together, leonurine suppressed the degradation of hemoglobin and inhibited microglia activation mainly through JNK pathway, which leads to maintain BBB function and ameliorate perihematomal edema.

Activated microglia also probably produce ROS to impair BBB function, which is considered an important step to the development of ICH (Sumi 2010). Further investigations are needed to clarify the exact antiapoptotic mechanism of leonurine during ICH, based on our present result of Tunel assay (Fig. 1E). In conclusion, it is discovered for the first time that leonurine can support BBB maintenance and decrease perihematomal edema to considerably protect brain tissue after ICH, indicating its potential as a new therapeutic approach for ICH treatment in the future.

4. Experimental

4.1. Animal preparation and experimental groups

Male Sprague-Dawley (SD) rats (240-260 g) were obtained from the Animal Research Center of Shanghai. Rats were divided into 6 groups: sham group, model group, mannitol-treated group (8 mg/kg/day, i.v.), leonurine-treated group (0.5 h and 2 h after operation, 15 mg/kg/day, i.v.). All protocols were in accordance with the Regulations of Ethical Standards and were approved by the Ethics Committee of Fudan University.

4.2. Cell culture and treatments

The immortalized Murine BV-2 microglial cell line, obtained from ATCC, was cultivated in DMEM (Hyclone, USA) supplemented with 10% FBS (Sigma, USA), 1% penicillin and streptomycin and 0.22 g/L sodium pyruvate at 37 °C in 5% CO_2 humidified atmosphere. BV-2 cells were pretreated in serum-free DMEM for 2 hours to reduce the effect of serum. To evaluate the protective effects of leonurine *in vitro*, BV-2 cells were treated with 10 μM OxyHb (Ruibio, O7109) in absence or presence of leonurine (0.3 μM - 10 μM) for 24 h.

4.3. ICH model

As previously reported, ICH was induced by a double autologous blood injection (Deinsberger et al. 1996). After SD rats were anesthetized and immobilized in a stereotactic frame, their bregma were exposed by 30% H_2O_2, and a 1 mm^2 burr hole was drilled by a dental drill in the skull (0.7 mm anterior to bregma and 3 mm lateral to midline). Each autologous blood sample was drawn from the caudal artery 30 s before injection. The autologous blood was inserted in the caudate putamen (5.8 mm deep) using a microsyringe, which was first injected at the rate of 3 μl/min for 5 min (15 μL of autologous blood), 10 min later followed by 35 μL injected over 7 min. The microsyringe was slowly withdrawn 30 min after the second injection. The sham group was only subjected to have a needle insertion.

4.4. Brain water content

Three days after ICH, rats were anesthetized by 10 % chloral hydrate. The brains were removed and separated into contralateral and ipsilateral hemispheres. These samples were placed in foil paper and wet weight was recorded immediately. After dried at 50 °C for 48 h, the dry weight of these samples were obtained by an electronic analytical balance. The formula for calculating BWC was as follows: (wet weight - dry weight)/ wet weight *100%.

4.5. Behavioral evaluation

As previously reported (Hua et al. 2002), SD rats were placed in a 2000 ml transparent beaker and a weight-shifting movement was initiated to contact the wall of beaker spontaneously. Under double-blinded conditions, an experimenter scored the behavior of the rats. The behavior was quantified under the occasions when the unimpaired forelimb was used to contact the wall. We analyzed the behavior 10 times and calculated the percentage according to the following formula: score = the number of using uninjured forelimbs / 10 * 100%.

4.6. Hematoxylin and eosin staining

Brain samples from SD rats were obtained through the perfusion of paraformaldehyde (PFA) 3 days after ICH. The samples were dehydrated at different concentrations of sucrose solution and embedded in paraffin. Paraffin sections of brain samples were stained by HE dye and detected as previously reported.

4.7. TUNEL staining

To visualize fragmented DNA of the apoptotic brain after ICH, a TUNEL assay was performed in accordance with *in situ* cell death detection kit fluorescein's instructions (Roche, USA). Paraffin sections of brain samples were covered by 50 μL TUNEL reaction mixture (enzyme solution and label solution, 1:50) and counterstained with DAPI for nuclear. Slides were directly observed by confocal laser scanning microscopy (Zeiss, Germany) and analyzed the percentage of apoptotic cells in the perihematoma.

4.8. Immunohistochemistry

The Paraffin sections of brain samples were treated with 0.01 M sodium citrate (pH=6.0) at 95 °C for 15 min. After blocking for 30 min at ambient temperature with 10% goat serum, sections were incubated with a goat polyclonal TLR4 antibody (Santa Cruz Biotechnology, USA) over night at 4 °C. Each section was incubated with 40 μL secondary antibody (Maixin, Fuzhou, China) for 4 h at ambient temperature, followed by staining with 3,3'-diaminobenzidine (DAB). Each section was visualized in the perihematoma by a Zeiss digital camera.

4.9. Evans Blue analysis

For analysis of the BBB permeability after ICH, SD rats were injected with 2% EB (4 ml/kg) into the tail vein and last for 4 h. After saline perfusion, the brain samples were removed and homogenized in trichloroacetic acid (TCA). The samples were centrifuged at 1000 rpm for 5 min.The supernatant was measured by the fluorescence reading at an excitation wavelength of 620 nm and an emission wavelength of 680nm. The EB content of each sample was determined with reference to a standard curve.

4.10. Cell viability

Cell viability was evaluated by CCK-8 assay. According to the product's instruction, BV-2 cells were seeded into 96-well plates (1×10^4 cells/well) and 10 μL CCK-8 (Dojindo, Japan) were added to each well after treatment. After incubation at 37 °C for 60 min, absorbance was measured at 450 nm and analyzed according to the following formula: cell viability = each group OD450 – blank OD450/ control OD450 - blank OD450.

4.11. Western blot analysis

Brain tissues or cells were lysed by RIPA buffer, and protein concentration of each group was determined by bicinchoninic acid (BCA) protein assay. Proteins were separated by 10% SDS-PAGE gel electrophoresis and then transferred to NC membranes. After blocking for 1.5 h at room temperature with 5% skim milk in TBST, the membranes were incubated with anti-MMP-2, anti-COX-2, anti-HO-1, anti-phospho-NF-κB, anti-NF-κB, anti-phospho-ERK1/2, anti- ERK1/2, anti-phospho-SAPK/JNK, anti-SAPK/JNK(1:1000, Cell Signaling Technology), anti-TLR4 (1:1000, Santa Cruz Biotechnology), anti-MyD88 (1:1000, AB Science), anti-GAPDH, anti-β-actin, anti-α-tubulin (1:10000, Proteintech) antibodies overnight at 4 °C. The membranes were washed by TBST three times (10 min each), and then incubated for an hour with secondary antibody (1:5000, Proteintech) at room temperature. Protein bands were quantitatively detected and analyzed by Image J software.

4.12. Determination of MMP-9 mRNA expression

Total RNA was extracted from injured brain tissues using Trizol reagent (TaKaRa, Japan) and then reverse transcribed into cDNAs. cDNAs of each sample were amplified with SYBR Green Master Mix and analyzed with GAPDH as control in the real-time PCR detection system iCycler iQ5 (Bio-Rad, CA). The primers were as follows:
MMP-9: 5'-GACCTCAAGTGGCACCATCA-3', 5'-AGTCATCGATCAC-GTCTCGC-3'
GAPDH: 5'-ATGTATCCGTTGTGGATCTGAC-3', 5'-CCTGCTTCAC-CACCTTCTTG-3'

4.13. Statistical analysis

Data were presented as mean±SEM. Graphpad software was used for statistical analysis. Statistical differences were analyzed using one-way analysis of variance (ANOVA) and compared using Student's *t*-test between two groups. $P < 0.05$ was considered statistically significant.

Acknowledgment: This work was supported by the grant from Specialized Research Fund for the Doctoral Program of Higher Education (No.20120071120048).

Conflicts of interest: None declared.

References

Adeoye O, Broderick JP (2010) Advances in the management of intracerebral hemorrhage. Nature Rev Neurol 6: 593-601.
Aronowski J, Zhao X (2011) Molecular pathophysiology of cerebral hemorrhage secondary brain injury. Stroke 42: 1781-1786.
Bodmer D, Vaughan KA, Zacharia BE, Hickman ZL, Connolly ES (2012) The molecular mechanisms that promote edema after intracerebral hemorrhage. Translat Stroke Res 3: 52-61.
Da Fonseca AC, Matias D, Garcia C, Amaral R, Geraldo L H, Freitas C, Lima FR (2014) The impact of microglial activation on blood-brain barrier in brain diseases. Front Cell Neurosci 8: 362-362.
Deinsberger W, Vogel J, Kuschinsky W, Auer LM, Boker DK (1996) Experimental intracerebral hemorrhage: Description of a double injection model in rats. Neurol Res 18: 475-477.
Gu Y, Zheng G, Xu M, Li Y, Chen X, Zhu W, Tong Y, Chung SK, Liu KJ, Shen J (2012) Caveolin-1 regulates nitric oxide-mediated matrix metalloproteinases activity and blood–brain barrier permeability in focal cerebral ischemia and reperfusion injury. J Neurochem 120: 147-156.
Hua Y, Schallert T, Keep RF, Wu J, Hoff JT, Xi G (2002) Behavioral tests after intracerebral hemorrhage in the rat. Stroke 33: 2478-2484.
James HE (2006) The effect of intravenous fluid replacement on the response to mannitol in experimental cerebral edema: an analysis of intracranial pressure, serum osmolality, serum electrolytes, and brain water content. Acta Neurochir Suppl. 96: 125-129.
Jie L, Xinchun J, Liu KJ, Wenlan L (2012) Matrix metalloproteinase-2-mediated occludin degradation and caveolin-1-mediated claudin-5 redistribution contribute to blood-brain barrier damage in early ischemic stroke stage. J Neurosc 32: 3044-3057.
Keep RF, Hua Y, Xi G (2012) Intracerebral haemorrhage: mechanisms of injury and therapeutic targets. Lancet Neurol 11: 720-731.
Lischper M, Beuck S, Thanabalasundaram G, Pieper C, Galla HJ (2010) Metalloproteinase mediated occludin cleavage in the cerebral microcapillary endothelium under pathological conditions. Brain Res 1326: 114-127.
Liu XH, Pan L, Wang X, Gong Q, Zhu YZ (2012) Leonurine protects against tumor necrosis factor-α-mediated inflammation in human umbilical vein endothelial cells. Atherosclerosis 222: 34-42.
Liu XH, Chen P-f, Pan L, De Silva R, Zhu YZ (2009) 4-Guanidino-n-butyl syringate (leonurine, SCM 198) protects H9c2 rat ventricular cells from hypoxia-induced apoptosis. J Cardiovasc Pharmacol 54: 437-444.
Liu XH, Pan LL, Chen PF, Zhu YZ (2010) Leonurine improves ischemia-induced myocardial injury through antioxidative activity. Phytomedicine 17: 753-759.
Nath FP, Jenkins A, Mendelow AD, Graham DI, Teasdale GM (1986) Early hemodynamic changes in experimental intracerebral hemorrhage. J Neurosurg 65: 697-703.
Qureshi AI, Ali Z, Suri MFK, Shuaib A, Baker G, Todd K, Guterman LR, Hopkins LN (2003) Extracellular glutamate and other amino acids in experimental intracerebral hemorrhage: an in vivo microdialysis study. Crit. Care Med 31: 1482-1489.
Sacco S, Marini C, Toni D, Olivieri L, Carolei A (2009) Incidence and 10-year survival of intracerebral hemorrhage in a population-based registry. Stroke 40: 394-399.
Strazza M, Pirrone V, Wigdahl B, Nonnemacher MR (2011) Breaking down the barrier: the effects of HIV-1 on the blood-brain barrier. Brain Res 1399: 96–115.
Sumi N, Nishioku T, Takata F, Matsumoto J, Watanabe T, Shuto H, et al. (2010) Lipopolysaccharide-activated microglia induce dysfunction of the blood-brain barrier in rat microvascular endothelial cells co-cultured with microglia. Cell Mol Neurobiol 30: 247–253.
Suzuki J, Imaizumi S, Kayama T, Yoshimoto T (1985) Chemiluminescence in hypoxic brain. The second report: cerebral protective effect of mannitol, vitamin E and glucocorticoid. Stroke 16: 695-700.
Ubenauf KM, Krueger, M., Henneke, P., and Berner, R (2007) Lipopolysaccharide binding protein is a potential marker for invasive bacterial infections in children. Pediatr Infect Dis J 26: 159-162.

Waleed B, Nancy S, El-Maraghy NN, Zakaria MNM (2014) Candesartan and glycyrrhizin ameliorate ischemic brain damage through downregulation of the TLR signaling cascade. Eur J Pharmacol 724: 43-50.

Xi G, Hua Y, Bhasin RR, Ennis SR, Keep RF, Hoff JT (2001) Mechanisms of edema formation after intracerebral hemorrhage: effects of extravasated red blood cells on blood flow and blood-brain barrier integrity. Stroke 32: 2932-2938.

Xi G, Keep RF, Hoff JT (2006) Mechanisms of brain injury after intracerebral haemorrhage. Lancet Neurol 5: 53-63.

Yang Y, Rosenberg GA (2011) MMP-mediated disruption of claudin-5 in the blood–brain barrier of Rat brain after cerebral ischemia. Methods Mol Biol 762: 333-345.

Yi Y, Estrada EY, Thompson JF, Wenlan L, Rosenberg GA (2007) Matrix metalloproteinase-mediated disruption of tight junction proteins in cerebral vessels is reversed by synthetic matrix metalloproteinase inhibitor in focal ischemia in rat. J Cereb Blood Flow Metab 27: 697-709.